



## Step-scan FTIR spectroscopy resolves the $Q_A^-Q_B \rightarrow Q_AQ_B^-$ transition in *Rb. sphaeroides* R26 reaction centres

Ronald Brudler & Klaus Gerwert\*

Lehrstuhl für Biophysik, Ruhr-Universität Bochum, Postfach 102148, 44780 Bochum, Germany; \*Author for correspondence

Received 11 August 1997; accepted in revised form 30 January 1998

**Key words:** electron-proton transfer, photosynthetic bacterial reaction centre, step-scan Fourier transform infrared spectroscopy, ubiquinone

### Abstract

It is shown that step-scan Fourier transform infrared spectroscopy can be applied to resolve the  $Q_A^-Q_B \rightarrow Q_AQ_B^-$  transition in *Rhodobacter sphaeroides* reaction centres with a 5  $\mu$ s time resolution. In the mid-infrared region (1900–1200  $\text{cm}^{-1}$ ), transient signals previously assigned to  $Q_{A/B}$  and  $Q_{A/B}^-$  vibrations, respectively (Brudler et al. 1994; Brudler et al. 1995; Breton and Navedryk 1996), can be resolved with this new technique. In addition, the three small positive bands in the spectral region of the carboxylic C=O stretching modes of acidic amino acid side chains are also resolved at 1730, 1719 and 1704  $\text{cm}^{-1}$ . A global fit analysis yields two exponentials with half-times of 150  $\mu$ s and 1.2 ms in agreement with IR spectroscopic studies at single wavenumbers (Hienerwadel et al. 1995), in the UV/VIS and near IR (Tiede et al. 1996, Li et al. 1996). The establishment of the step-scan technique enables a new approach to elucidate the molecular mechanism of this transition.

**Abbreviations:** FTIR – Fourier transform infrared;  $H_A$  – intermediary electron acceptor; IR – infrared; MIR – mid-infrared; P – primary electron donor;  $Q_A$  – primary acceptor quinone;  $Q_B$  – secondary acceptor quinone; RC – reaction centre; *Rb.* – *Rhodobacter*; UQ – ubiquinone; vis – visible

### Introduction

In the photosynthetic reaction centre (RC) of *Rhodobacter sphaeroides*, light excitation induces a transmembrane charge separation originating at the primary donor P (bacteriochlorophyll *a*-dimer), proceeding via  $H_A$  (bacteriopheophytin *a*) and  $Q_A$  (ubiquinone-10 = UQ<sub>10</sub>) and terminating at  $Q_B$  (UQ<sub>10</sub>). FTIR difference spectra ( $P^+Q_A^- - PQ_A$ ,  $P^+Q_B^- - PQ_B$ ,  $H_A^- - H_A$ ,  $Q_A^- - Q_A$ ,  $Q_B^- - Q_B$ ) between a charge separated state stabilized by continuous illumination and the neutral ground state have been recorded to study the molecular reactions of the cofactors and the protein environment involved in the electron transfer (Gerwert 1993; Mäntele 1993; Navedryk 1996). Specific band assignments were recently achieved for the  $Q_A$  and  $Q_B$  and the  $Q_A^-$  and  $Q_B^-$  vibrations by site-specific <sup>13</sup>C-labelling of

ubiquinone and reconstitution at the  $Q_A$  and  $Q_B$  binding site, respectively (Breton et al. 1994, 1995; Brudler et al. 1994, 1995).

While steady-state FTIR difference spectroscopy monitors the molecular changes in the respective relaxed states, time-resolved IR spectroscopy must be applied to investigate the transient processes. Taking advantage of the different recombination lifetimes of the photoinduced intermediates  $P^+Q_A^-$  (~100 ms) and  $P^+Q_B^-$  (~1 s) a  $Q_A^-Q_B - Q_AQ_B^-$  double difference spectrum was calculated using the rapid-scan FTIR technique with a 25 ms time resolution (Thibodeau et al. 1990). Direct investigation of the  $Q_A^-Q_B \rightarrow Q_AQ_B^-$  transition which takes place in 200  $\mu$ s (Vermeglio and Clayton 1977) was performed at single frequencies with tunable IR laser diodes with 0.5  $\mu$ s time resolution (Hienerwadel et al. 1992; Hienerwadel et al. 1995). Stroboscopic FTIR spec-

trospectroscopy with a time resolution of 25  $\mu\text{s}$  (Souvignier and Gerwert 1992) and the step-scan FTIR technique with a time resolution of up to 10 ns (Uhlmann et al. 1991; Rammelsberg et al. 1997) enable simultaneous data acquisition in the whole MIR range. Only the complete IR difference spectra allow unequivocal band assignments and thereby a complete description of the molecular changes. Burie et al. (1993) have used the step-scan method with a 10  $\mu\text{s}$  time-resolution to investigate the  $\text{PQ}_A$  to  $\text{P}^+\text{Q}_A^-$  and the P to  $^3\text{P}$  transitions. Here we describe the first step-scan investigation of the  $\text{Q}_A^-\text{Q}_B \rightarrow \text{Q}_A\text{Q}_B^-$  transition with a 5  $\mu\text{s}$  time resolution. The absorbance changes of this transition are much smaller than for the  $\text{P}^+\text{Q}_A^-$  transition and demand improved S/N.

### Materials and methods

The experiments were performed on a vacuum FTIR spectrometer (IFS 66v, Bruker) with a globar IR source, KBr beamsplitter and MCT detector. The scanner stability was determined to be  $\pm 1$  nm (Rammelsberg et al. 1997).

The spectra were recorded between 1975 – 988  $\text{cm}^{-1}$  with a resolution of 7  $\text{cm}^{-1}$ ; the resolution of the phase spectrum was 50  $\text{cm}^{-1}$ . At each scanner position 1000 time points spaced by 5  $\mu\text{s}$  were collected. The reaction was started 60  $\mu\text{s}$  after the scanner's stop by a laser flash (540 nm, 20 ns,  $\sim 5$  mJ). The laser flashes were separated by 20 s to ensure full recombination from the charge separated state to the neutral ground state of the RC. In order to improve the S/N ratio, 24 measurements on one sample were averaged. The duration of one measurement was 1.5 h. Between the measurements, static  $\text{P}^+\text{Q}_B^- - \text{PQ}_B$  difference spectra were recorded in order to control the activity of the protein. The reconstruction of the interferograms and the computation of the difference spectra were carried out with the OPUS software from Bruker. The interferograms were multiplied with the 'Norton-Beer, weak' apodization function and zero-filled by a factor of 4. Phase correction was done by the Mertz method. The resulting 1000 difference spectra were averaged on a logarithmic time scale.

The principles and experimental details of the FTIR step-scan measurement are described in Rammelsberg et al. (1997).

The kinetic analysis was performed using the 'Global Fit' program (Heßling et al. 1993) taking into account absorbance changes of the complete spectra.

In order to eliminate the dominant  $\text{P}^+/\text{P}$  bands that mask the (semi) quinone and protein vibrations and to remove contributions from the  $\text{P}^+\text{Q}_A^- \rightarrow \text{PQ}_A$  recombination kinetics, the first difference spectrum ( $\text{P}^+\text{Q}_A^- - \text{PQ}_A$ ) recorded 7  $\mu\text{s}$  after the laser flash was subtracted from the following difference spectra. For subtraction the spectra were normalized on the whole frequency range from 1975 to 988  $\text{cm}^{-1}$ . A satisfactory fit resulted in a random distribution of the residuals around the zero-line, a standard deviation close to 1 (1.06) and a minor correlation of the rate constants. For the steady-state  $\text{P}^+\text{Q}_A^- - \text{PQ}_A$  difference spectrum, 6400 interferograms with a spectral resolution of 4  $\text{cm}^{-1}$  were recorded before and during continuous illumination with a halogen lamp. Therefore, the S/N is about 16 fold increased as compared to the time-resolved difference spectra.

RC protein was purified from *Rb. sphaeroides* strain R26 and reconstituted with a 20 fold excess of  $\text{UQ}_2$  at the  $\text{Q}_B$  site (Okamura et al. 1975). 36  $\mu\text{l}$  RC solution (10 mM Tris, 0.025% LDAO, 1 mM EDTA, pH 8) with  $\text{OD}_{802} = 20$  was dried on a  $\text{CaF}_2$  window under a gentle stream of nitrogen, rehydrated, covered with another  $\text{CaF}_2$  window and thermostabilized at 22  $^\circ\text{C}$  in the spectrometer.

### Results and discussion

Figure 1a shows a  $\text{P}^+\text{Q}_A^- - \text{PQ}_A$  difference spectrum, recorded with the step-scan method 7  $\mu\text{s}$  after the laser flash. For comparison, a  $\text{P}^+\text{Q}_A^- - \text{PQ}_A$  difference spectrum generated under continuous illumination with a halogen lamp is shown in Figure 1b. Both difference spectra agree well. The noise amplitudes of the step-scan measurement and the static measurement can be compared between 1900–1800  $\text{cm}^{-1}$ . It should be noted that the difference spectra in Figure 1 do not have to agree completely since the step-scan spectrum reflects a transient state during electron transfer and the static spectrum represents a fully relaxed state after electron transfer. In the following only signals larger than  $10^{-3}$  absorbance units, that are clearly above the noise level, are discussed. The difference spectrum in Figure 1a reveals all the bands that are typical for the  $\text{PQ}_A \rightarrow \text{P}^+\text{Q}_A^-$  transition. The difference spectra agree also nicely with the one measured in Burie et al. (1993). Some bands have been tentatively assigned in static  $\text{P}^+\text{Q}_A^- - \text{PQ}_A$  and  $\text{P}^+ - \text{P}$  difference spectra by comparison with model compounds (Gerwert et al. 1988; Mäntele et al. 1988; Buchanan et al.



1992; Leonhard and Mäntele 1993; Nabedryk 1996). The differential signal at 1753/1743  $\text{cm}^{-1}$  (Figure 1a) was suggested to arise from the 10a-ester C=O groups of  $\text{P}^+$  and P, respectively. The positive bands at 1716 and 1706  $\text{cm}^{-1}$  in Figure 1a (1716 and 1705  $\text{cm}^{-1}$  in Figure 1b) are most probably due to the two 9-keto C=O groups of  $\text{P}^+$ ; the negative bands at 1692 and 1683  $\text{cm}^{-1}$  (Figure 1b) have been assigned to the 9-keto C=O groups of P (Nabedryk, 1996). The reason why the band at 1683  $\text{cm}^{-1}$  appears only as a small shoulder (Figure 1a) and the intensities of the signals at 1692 and 1683  $\text{cm}^{-1}$  in Figure 1a are inverse as compared to Figure 1b is not yet clear. In another step-scan measurement these bands agree with the static difference spectra. A band at  $\sim 1665 \text{ cm}^{-1}$  (corresponding to the band at 1669  $\text{cm}^{-1}$  in Figure 1b), previously assigned to a 9-keto C=O group of P (Mäntele et al. 1988), more probably is due to a peptide C=O in the environment of P (Nabedryk 1996). The band at 1627  $\text{cm}^{-1}$  in Figure 1a (1630  $\text{cm}^{-1}$  in Figure 1b) arises partly from the coupled C=O/C=C stretching vibration of  $\text{Q}_\text{A}$  (Brudler et al. 1994). Contributions from the 2a-acetyl C=O groups of P must be also taken into account in this spectral region (Leonhard and Mäntele 1993). In addition, the positive signals at 1568, 1545, 1479, 1462, 1402 and 1296  $\text{cm}^{-1}$  (Figure 1a) have clear correspondences in the static difference spectrum (Figure 1b) and can be attributed mainly to  $\text{P}^+$  (Leonhard and Mäntele 1993). Between 1470–1440  $\text{cm}^{-1}$ ,  $\text{Q}_\text{A}^-$  vibrations have been identified at 1486, 1466 and 1447  $\text{cm}^{-1}$  (see below).

Figure 2a compares the time resolved  $\text{P}^+\text{Q}_\text{A}^- - \text{PQ}_\text{A}$  difference spectrum from Figure 1a 7  $\mu\text{s}$  after the laser flash with a difference spectrum recorded 4.2 ms after the reaction's start ( $= \text{P}^+\text{Q}_\text{B}^- - \text{PQ}_\text{B}$ ; Figure 2b). Both spectra are very similar and are dominated by the  $\text{P}^+/\text{P}$  bands. This indicates that after 7  $\mu\text{s}$  no reactions that lead to a redistribution of electron density on the primary donor take place. However, the S/N is not improved at 4.2 ms as expected. The noise is not determined by the detector, but due to specificities of the step-scan measurement (e.g. the scanner stability). Small differences between the two spectra are seen mainly between 1670–1600  $\text{cm}^{-1}$  (C=O and C=C stretching vibrations of  $\text{Q}_\text{A}$  and  $\text{Q}_\text{B}$ ) and 1500–1400  $\text{cm}^{-1}$  (C=O and C=C stretching vibrations of  $\text{Q}_\text{A}^-$  and  $\text{Q}_\text{B}^-$ ). To visualize more clearly these deviations, the  $\text{P}^+\text{Q}_\text{B}^- - \text{PQ}_\text{B}$  spectrum was subtracted from the  $\text{P}^+\text{Q}_\text{A}^- - \text{PQ}_\text{A}$  spectrum. In the resulting  $\text{Q}_\text{A}^- \text{Q}_\text{B} - \text{Q}_\text{A} \text{Q}_\text{B}^-$  double difference spectrum (Figure 2c), the  $\text{P}^+$  and P bands are eliminated;

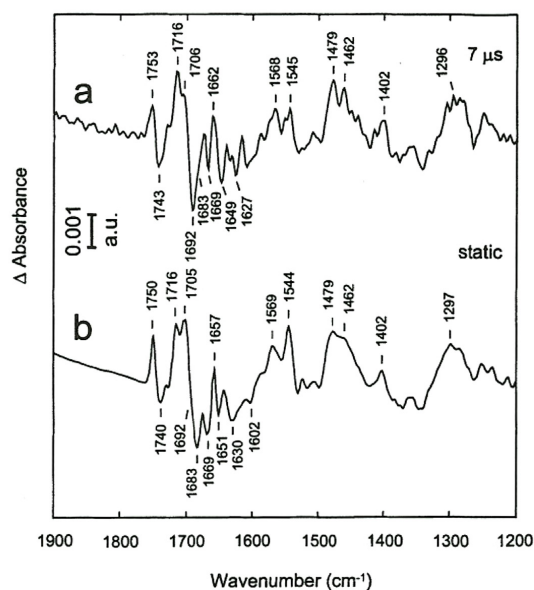


Figure 1.  $\text{P}^+\text{Q}_\text{A}^- - \text{PQ}_\text{A}$  difference spectra. (a) measured with the step-scan method 7  $\mu\text{s}$  after the laser flash, (b) statically measured under continuous illumination with a halogen lamp.

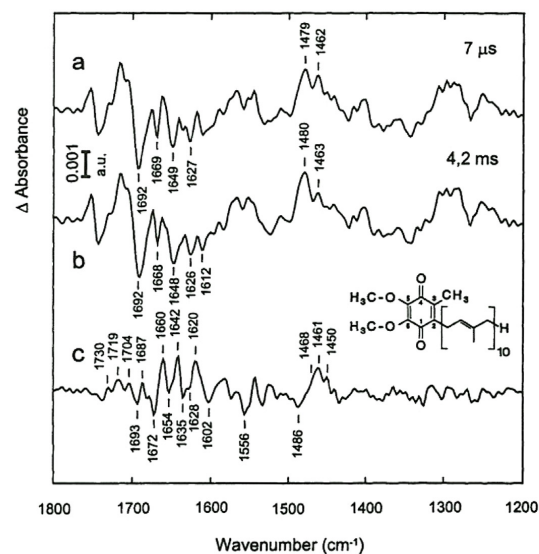


Figure 2. (a) Difference spectrum, recorded 7  $\mu\text{s}$  after the laser flash:  $\text{P}^+\text{Q}_\text{A}^- - \text{PQ}_\text{A}$  (b) Difference spectrum, recorded 4.2 ms after the laser flash:  $\text{P}^+\text{Q}_\text{B}^- - \text{PQ}_\text{B}$ . (c) Double difference spectrum (b-a):  $\text{Q}_\text{A}^- \text{Q}_\text{B} - \text{Q}_\text{A} \text{Q}_\text{B}^-$ . Inset: Structural formula and IUPAC numbering of ubiquinone-10.

the positive bands belong to  $Q_A^-$  or  $Q_B$  and the negative bands to  $Q_B^-$  or  $Q_A$ . Besides the bands deriving from the (semi) quinones, vibrations of the protein backbone and of the protein's side chains contribute to the double difference spectrum. By use of site-specific  $^{13}\text{C}$ -labelled  $\text{UQ}_{10}$  (Brudler et al. 1994, 1995) and reconstitution at the  $Q_A$  and  $Q_B$  site, respectively, the  $\text{C}=\text{O}$  and  $\text{C}=\text{C}$  stretching vibrations of  $Q_A$  and  $Q_B$  and the  $\text{C}\equiv\text{O}$  and  $\text{C}\equiv\text{C}$  stretching vibrations of  $Q_A^-$  and  $Q_B^-$  have been assigned. They can be found in the double difference spectrum of Figure 2c. The positive band at  $1642\text{ cm}^{-1}$  is caused by the 1- and 4- $\text{C}=\text{O}$  stretching vibration of  $Q_B$ . The negative band at  $1628\text{ cm}^{-1}$  represents a coupled  $\text{C}=\text{O}/\text{C}=\text{C}$  stretching mode of  $Q_A$ . A broad positive band at  $1620\text{ cm}^{-1}$  contains the  $\text{C}=\text{C}$  stretching vibration of  $Q_B$ . The 4- $\text{C}=\text{O}$  group of  $Q_A$  absorbs mainly at  $1602\text{ cm}^{-1}$ . The 1- $\text{C}=\text{O}$  group of  $Q_A$  absorbs at  $1660\text{ cm}^{-1}$  (Brudler et al. 1994) and should appear as a negative band in Figure 2c. Instead, a strong positive band which is not yet assigned is found at  $1660\text{ cm}^{-1}$  in the double difference spectrum that masks the negative signal of the 1- $\text{C}=\text{O}$  group.

Specific band assignments are more difficult to perform for the semiquinone vibrations ( $1500 - 1400\text{ cm}^{-1}$ ) because the bands overlap more than for the neutral quinones. In addition, the  $\text{C}\equiv\text{O}$  vibrations of the two carbonyl groups of  $Q_A^-$  are coupled, in contrast to the  $\text{C}=\text{O}$  vibrations of  $Q_A$ . Also coupling between the  $\text{C}\equiv\text{O}$  and  $\text{C}\equiv\text{C}$  modes is enhanced due to the increased aromatic character of the molecule (Chipman and Prebenda 1986; Brudler et al. 1994). While there is an excellent agreement for the assignments of the  $Q_A$  vibrations, different assignments have been reported for  $Q_A^-$  (compare Brudler et al. 1994 and Breton and Navedryk 1996). It therefore should be stressed that a normal mode analysis and further site-specific isotope labelling are necessary to clarify the deviations. In the double difference spectrum of Figure 2c, three positive bands occur at  $1468$ ,  $1461$  and  $1450\text{ cm}^{-1}$  which are characteristic of  $Q_A^-$  (see for example Brudler et al. 1994). The band at  $1468\text{ cm}^{-1}$  was assigned to a predominant 4- $\text{C}\equiv\text{O}$  stretching mode and the band at  $1450\text{ cm}^{-1}$  (corresponding most probably to the band at  $1447\text{ cm}^{-1}$  in Brudler et al. 1994) to a  $\text{C}\equiv\text{C}$  mode with a high degree of the 1- and 4- $\text{C}\equiv\text{O}$  stretching vibrations. A broad negative band with a minimum at  $1486\text{ cm}^{-1}$  (Figure 2c) contains the 1- and 4- $\text{C}\equiv\text{O}$  stretching vibrations of  $Q_B^-$  (Brudler et al. 1995). The amplitude of this band is probably decreased by a  $Q_A^-$  band

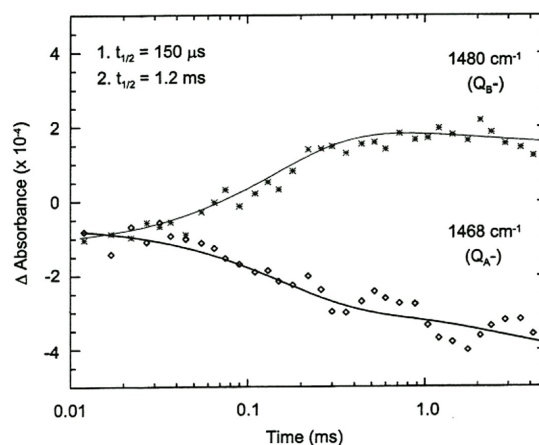


Figure 3. Kinetics at  $1480\text{ cm}^{-1}$  (1- and 4- $\text{C}\equiv\text{O}$  stretching vibrations of  $Q_B^-$ ) and  $1468\text{ cm}^{-1}$  (4- $\text{C}\equiv\text{O}$  stretching vibration of  $Q_A^-$ ).

absorbing at  $1486\text{ cm}^{-1}$ , previously assigned to the 1- $\text{C}\equiv\text{O}$  stretching vibration of  $Q_A^-$  (Brudler et al. 1994).

Unspecific incorporation of  $1'\text{-}^{15}\text{N}$ -labelled Trp in the RC has revealed a signal at  $1553\text{ cm}^{-1}$  (Brudler 1996). The band at  $1556\text{ cm}^{-1}$  (Figure 2c) therefore is (partly) assigned to Trp, most probably to Trp M252 which is in van-der-Waals contact with  $Q_A$  (Ermler et al. 1994). In the spectral region of the carboxylic  $\text{C}=\text{O}$  stretching modes of acidic amino acid side chains ( $1780 - 1690\text{ cm}^{-1}$ ), three small bands at  $1730$ ,  $1719$  and  $1704\text{ cm}^{-1}$  are resolved (Figure 2c). Hienerwadel et al. (1995) have described three corresponding bands at  $1732$ ,  $1725$  and  $1706\text{ cm}^{-1}$ . On the basis of  $^1\text{H} \rightarrow ^2\text{H}$  exchange and a Glu L212 Gln mutant, they have assigned the band at  $1725\text{ cm}^{-1}$  (most probably corresponding to the band at  $1719\text{ cm}^{-1}$  in Figure 2c) to the  $\text{COOH}$  group of Glu L212.

The appearance of the typical  $Q_{A/B}$  and  $Q_{A/B}^-$  bands in the double difference spectrum (Figure 2c) can be taken as evidence for the correct time and amplitude resolved detection of the  $Q_A^-Q_B \rightarrow Q_AQ_B^-$  transition by step-scan FTIR difference spectroscopy. For the kinetic analysis, the  $\text{P}^+Q_A^- - \text{P}Q_A$  difference spectrum generated 7 after the flash was subtracted from the following difference spectra (see materials and methods). The analysis shows that a sum of two exponentials with half-times of  $150\text{ }\mu\text{s}$  and  $1.2\text{ ms}$  was sufficient for a satisfactory description at all wavenumbers. Figure 3 shows two representative kinetics, at  $1480\text{ cm}^{-1}$  (appearance of  $Q_B^-$ ) and at  $1468\text{ cm}^{-1}$  (disappearance of  $Q_A^-$ ). The kinetics



show that the absorbance changes can be followed time-resolved. However, there is a small oscillation superimposed, which seems to be an artefact.

Heterogenous  $Q_A^-Q_B \rightarrow Q_AQ_B^-$  electron transfer rates have been observed by several groups in the IR and Vis spectral region (Hienerwadel et al. 1995; Tiede et al. 1995; Li et al. 1996). Hienerwadel et al. (1995) have characterized the  $Q_A^-Q_B \rightarrow Q_AQ_B^-$  transition between  $1780 - 1690 \text{ cm}^{-1}$  with a time resolution of  $0.5 \mu\text{s}$  and a spectral resolution of  $4 - 5 \text{ cm}^{-1}$  with tunable diode lasers. A global fit analysis yielded half-times of  $180 \mu\text{s}$  and  $1.05 \text{ ms}$  in good agreement with the published data. In contrast to the results of Hienerwadel et al. (1992), the different spectral regions representing different molecular groups can be described with the same rate constants and no hint of a different protein kinetic as compared to the chromophores is seen.

The fast rate could simply represent electron transfer and the slow rate proton transfer. But this seems unlikely because the  $Q_A^-$  band shows also the slow component. This band should not be observed during the proton uptake. In an alternative explanation the two rates could be related to different RC conformations at the  $Q_A$  and/or  $Q_B$  binding site, resulting in polyphasic kinetics for the different conformational states. In a third model the slow phase could be explained by a movement of  $Q_B$  from an inactive to an active position, as revealed recently by X-ray crystallography (Stowell et al. 1997). This model is in agreement with the finding of two different  $UQ_{10}$  positions at the  $Q_B$  site (Brudler et al. 1995). However, to discuss the results of the step-scan measurement more detailed, we have to improve the S/N ratio by averaging more samples. This experiments are in progress using an improved experimental setup with  $30 \text{ ns}$  time-resolution (Rammelsberg et al. 1997).

By establishing the step-scan technique on photosynthetic reaction centres, we opened now the door for further studies on the  $Q_A^-Q_BQ_AQ_B^-$  transition in which complete mid IR spectra can be obtained in  $30 \text{ ns}$ . By use of site-specifically mutated and isotopically labeled RCs this will allow unequivocal band assignments as prerequisite for the understanding of the molecular reaction mechanisms of this transition.

## Acknowledgements

Robin Rammelsberg is gratefully acknowledged for technical help. This work was supported by the Deutsche Forschungsgemeinschaft (SFB 480-C3).

## References

- Breton J, Boullais C, Burie J-R, Nabadryk E and Mioskowski C (1994) Binding sites of quinones in photosynthetic bacterial reaction centers investigated by light-induced FTIR difference spectroscopy: Assignment of the interactions of each carbonyl of  $Q_A$  in *Rhodobacter sphaeroides* using site-specific  $^{13}\text{C}$ -labeled ubiquinone. *Biochemistry* 33: 14378–14386
- Breton J, Boullais C, Berger G, Mioskowski C and Nabadryk E (1995) Binding sites of quinones in photosynthetic bacterial reaction centers investigated by light-induced FTIR difference spectroscopy: Symmetry of the carbonyl interactions and close equivalence of the  $Q_B$  vibrations in *Rhodobacter sphaeroides* and *Rhodospseudomonas viridis* probed by isotope labeling. *Biochemistry* 34: 11606–11616
- Breton J and Nabadryk E (1996) Protein-quinone interactions in the bacterial photosynthetic reaction center: light-induced FTIR difference spectroscopy of the quinone vibrations. *Biochim Biophys Acta* 1275: 84–90
- Brudler R, de Groot HJM, van Liemt WBS, Steggerda WF, Esmeijer R, Gast P, Hoff AJ, Lugtenburg J and Gerwert K (1994) Asymmetric binding of the 1- and 4-C=O groups of  $Q_A$  in *Rhodobacter sphaeroides* R26 reaction centres monitored by Fourier transform infra-red spectroscopy using site-specific isotopically labelled ubiquinone-10. *EMBO J* 13: 5523–5530
- Brudler R, de Groot HJM, van Liemt WBS, Gast P, Hoff AJ, Lugtenburg J and Gerwert K (1995) FTIR spectroscopy shows weak symmetric hydrogen bonding of the  $Q_B$  carbonyl groups in *Rhodobacter sphaeroides* R26 reaction centres. *FEBS Lett* 370: 88–92
- Brudler R (1996) Charakterisierung der Chinonbindestellen im photosynthetischen Reaktionszentrum von *Rhodobacter sphaeroides* mit Hilfe von statischer und zeitaufgelöster FTIR-Differenzspektroskopie. PhD thesis, Ruhr-Universität-Bochum
- Buchanan S, Michel H and Gerwert K (1992) Light-induced charge separation in *Rps. viridis* reaction centers monitored by FTIR difference spectroscopy: the Quinone vibrations. *Biochemistry* 31: 1314–1322
- Burie J-R, Leibl W, Nabadryk E and Breton J (1993) Step-scan FT-IR spectroscopy of electron transfer in the photosynthetic bacterial reaction center. *Appl Spectrosc* 47: 1401–1404
- Chipman DM and Prebenda MF (1986) Structures and fundamental vibrations of p-benzoquinone and p-benzoquinone radical anion from ab initio calculations. *J Phys Chem* 90: 5557–5560
- Ermeler U, Fritsch G, Buchanan S and Michel H (1994) Structure of the photosynthetic reaction centre from *Rhodobacter sphaeroides* at  $2.65 \text{ \AA}$  resolution: cofactors and protein-cofactor interactions. *Structure* 2: 925–936
- Gerwert K, Hess B, Michel H and Buchanan S (1988) FTIR studies on crystals of photosynthetic reaction centers. *FEBS Lett* 232: 303–307
- Gerwert K (1993) Molecular reaction mechanisms of proteins as monitored by time-resolved FTIR spectroscopy. *Curr Opin Struct Biol* 3: 769–773

- Heßling B, Souvignier G and Gerwert K (1993) A model-independent approach to assigning bacteriorhodopsin's intramolecular reactions to photocycle intermediates. *Biophys J* 65: 1929–1941
- Hienerwadel R, Thibodeau D, Lenz F, Nabadryk E, Breton J, Kreutz W and Mäntele W (1992) Time-resolved infrared spectroscopy of electron transfer in bacterial photosynthetic reaction centers: Dynamics of binding and interaction upon  $Q_A$  and  $Q_B$  reduction. *Biochemistry* 31: 5799–5808
- Hienerwadel R, Grzybek S, Fogel C, Kreutz W, Okamura MY, Paddock ML, Breton J, Nabadryk E and Mäntele W (1995) Protonation of Glu L212 following  $Q_B^-$  formation in the photosynthetic reaction center of *Rhodobacter sphaeroides*: Evidence from time-resolved infrared spectroscopy. *Biochemistry* 34: 2832–2843
- Leonhard M and Mäntele W (1993) Fourier transform infrared spectroscopy and electrochemistry of the primary electron donor in *Rhodobacter sphaeroides* and *Rhodopseudomonas viridis* reaction centers: Vibrational modes of the pigments in situ and evidence for protein and water modes affected by  $P^+$  formation. *Biochemistry* 32: 4532–4538
- Li J, Gilroy D and Gunner MR (1996) The rate of electron transfer from  $D^+Q_A^-Q_B$  to  $D^+Q_AQ_B^-$  in *Rb. sphaeroides* reaction centers. *Biophys J* 70: A10
- Mäntele WG, Wollenweber AM, Nabadryk E and Breton J (1988) Infrared spectroelectrochemistry of bacteriochlorophylls and bacteriopheophytins: Implications for the binding of the pigments in the reaction center from photosynthetic bacteria. *Proc Natl Acad Sci USA* 85: 8468–8472
- Mäntele W (1993) Infrared vibrational spectroscopy of the photosynthetic reaction center. In: Deisenhofer J and Norris J (eds) *The Photosynthetic Reaction Center*, pp 239–283. Academic Press, New York
- Nabadryk E (1996) Light-induced Fourier transform infrared difference spectroscopy of the primary electron donor in photosynthetic reaction centers. In: Mantsch H and Chapman D (eds) *Infrared Spectroscopy of Biomolecules*, pp 39–81. Wiley-Liss Inc.
- Okamura MY, Isaacson RA and Feher G (1975) Primary acceptor in bacterial photosynthesis: Obligatory role of ubiquinone in photoactive reaction centers of *Rhodopseudomonas sphaeroides*. *Proc Natl Acad Sci USA* 72: 3491–3495
- Rammelsberg R, Heßling B, Chorogiewski H and Gerwert K (1997) Molecular reaction mechanisms of proteins monitored by nanosecond step-scan FT-IR difference spectroscopy. *Appl Spectrosc* 51: 558–562
- Souvignier G and Gerwert K (1992) Proton uptake mechanism of bacteriorhodopsin as determined by time-resolved stroboscopic FTIR-spectroscopy. *Biophys J* 63: 1393–1405
- Stowell MHB, McPhillips TM, Rees DC, Soltis SM, Abresch E and Feher G (1997) Light-induced structural changes in photosynthetic reaction center: Implications for mechanism of electron-proton transfer. *Science* 276: 812–816
- Thibodeau DL, Nabadryk E, Hienerwadel R, Lenz F, Mäntele W and Breton J (1990) Time-resolved FTIR spectroscopy of quinones in *Rb. sphaeroides* reaction centers. *Biochim Biophys Acta* 1020: 253–259
- Tiede DM, Vázquez J, Córdova J and Marone PA (1996) Time-resolved electrochromism associated with the formation of quinone anions in the *Rhodobacter sphaeroides* R26 reaction center. *Biochemistry* 35: 10763–10775
- Uhlmann W, Becker A, Taran C and Siebert F (1991) Time-resolved FT-IR absorption spectroscopy using a step-scan interferometer. *Appl Spectrosc* 45: 390–397
- Vermeglio A and Clayton RK (1977) Kinetics of electron transfer between the primary and the secondary electron acceptor in reaction centers from *Rhodopseudomonas sphaeroides*. *Biochim Biophys Acta* 461: 159–165